Effect of germination on the functional and moisture sorption properties of high pressure processed foxtail millet grain flour

Article

Accepted Version

Effect of germination on the functional and moisture sorption properties of high pressure processed foxtail millet grain flour

Nitya Sharma[a]*, S.K. Goyal[a], Tanweer Alam[b], Sana Fatma[c], Keshavan Niranjan[d]

[a]Department of Farm Engineering, Institute of Agricultural Sciences, Banaras Hindu University, Varanasi (India)

[b]Indian Institute of Packaging, New Delhi (India)

[c]Centre of Food Science and Technology, Banaras Hindu University, Varanasi (India)

[d]Department of Food and Nutritional Sciences, University of Reading, Reading (UK)

* Corresponding author email ID: nitya.sharma64@gmail.com

Abstract Foxtail millet is one of the commonly cultivated, nutritionally competitive source of protein, fibre, phytochemicals and other micronutrients, as compared to major cereals like wheat and rice. Considering the potential of these grains, the high pressure processed flours of germinated (GFMF) and non-germinated foxtail millet (NGFMF) grains were studied for its functional, moisture sorption and thermodynamic properties. Germination and high pressure processing of foxtail millet grains significantly improved the functional properties of the flour. Apart from this, the moisture sorption isotherms of both the flours were determined at 10, 25 and 40 ^{o}C and the sorption data was fitted to Guggenheim-Anderson-De Boer (GAB) sorption model. The monolayer moisture content for NGFMF and GFMF ranged between 3.235 - 2.364 g g^{-1} and 2.987 – 2.063 g g^{-1}, respectively. The isosteric heat of sorption ranged between -76.35 kJ mol^{-1} to -38.23 kJ mol^{-1} for NGFMF and 172.55 kJ mol^{-1} to -34.02 kJ mol^{-1} for GFMF at a moisture range of 0 to 36%, whereas, the integral entropy of sorption for NGFMF ranged between -0.404 to -0.120 kJ mol^{-1} K^{-1} and for GFMF between -0.667 to -0.383 kJ mol^{-1} K^{-1}. Along with the validation of the compensation theory, the values of spreading pressures lied in the range of 0 – 0.078 J m^{-2} for NGFMF and 0 – 0.124 J m^{-2} for GFMF, while, the glass transition temperatures ranged between 82.25 to 28.67 ^{o}C for NGFMF and from 51.11 to 11.83 ^{o}C for GFMF at all three temperatures.

Keywords Foxtail millet flour, germination, high pressure processing, functional properties, moisture sorption isotherms, thermodynamic properties

Introduction

Water sorption characteristics are necessary for predicting the shelf life and determining the moisture content and critical activity for acceptability of products that deteriorate, mainly due to moisture gain, and also for drying, packaging and storage (Katz and Labuza 1981). A food moisture sorption isotherm describes the relationship between the moisture uptake in food and the relative humidity of the air with which the food is in equilibrium at a constant temperature (Lagoudaki et al. 1993). Thermodynamics has been reported as an approach to understand the properties of water and calculate the energy requirements of heat and mass transfer in biological systems (Rizvi and Benado 1983; Fasina et al. 1997; Fasina et al. 1999). Properties such as isosteric heat of sorption, net integral enthalpy and entropy and spreading pressures are important for understanding the energy requirement during dehydration, the food microstructure, physical phenomena on the food surfaces and sorption kinetic parameters (Rizvi and Benado 1983). Also, the glass transition temperature is an important physical parameter, which serves to explain the physical and chemical behaviour of food systems (Bell and Labuza 2000), and it is defined as the temperature at which the material changes from the glassy to the rubbery state for a given heating rate.

Foxtail millet (*Setaria italica* (L.) P. Beauv.) is the sixth highest yielding grain amongst all the millet varieties and has been identified as a major millet in terms of worldwide production (Sharma et al. 2017). Foxtail millet ranks second in the total world millet production of around 29 million tonnes (in 2015-16 season). It originates in the Yellow River Basin country, which makes China a leading foxtail millet producer holding 80% of world production, followed by India with 10% of world production (Zhang et al. 2017). Foxtail millet is one of the oldest cultivated cereal grains belonging to the *Setaria* genus, of *Poaceae* family and subfamily *Panicoideae*. Sharma et al. (2017) have discussed the versatility of foxtail millet as a food source and its potential to address food and nutrition security. These authors have reviewed the effects of various processing techniques on the properties of foxtail millet grains.

It has been recognised that non-thermal processing techniques like high hydrostatic pressures (HHP), can potentially inactivate anti-nutritional factors like phytate and tannin content in cereal grains and preserve their constituents and quality (Estrada-Girón et al. 2005; Yu et al. 2015; Zhang et al. 2017). In addition to high pressure processing, germination, is one of the traditional approaches used to supplement the bio-accessibility of nutrients in plant-based

diets. The process of germination in cereal grains results in an increase in enzymatic activity, soluble protein content and break down of starch into simple sugars, resulting in the formation of typical colours and flavours (Barreiro et al. 2003). Moisture sorption properties have also been studied for various cereals and its products like various cereal grains and legumes (Al-Mahasneh et al. 2014), milk-foxtail millet powder (Simha et al. 2016), two millet grain varieties (Aviara et al. 2016), tef (*Eragrostis tef* (Zucc.) Trotter) grain flour (Abebe and Ronda 2015), bulgar (Erbaş et al. 2015), Greek durum wheat semolina (Pollatos et al. 2013), RTE breakfast cereal formulation (Sandoval et al. 2009), oat and rice flour (Brett et al. 2009), maize meal and millet flours (Ikhu-Ornoregbe and Chen 2005). In general, very limited moisture sorption data is available for germinated cereals, especially for high pressure processed and germinated millet grains. This study was therefore conducted to assess the effect of germination on the functional, moisture sorption and thermodynamic properties of high pressure processed foxtail millet grain flour.

Materials and methods

Sample collection

Foxtail millet (*Setaria italica* L.) grains were procured from authorized grain centres. All procured grains were a month old since harvesting and were tested for viability using tetrazolium chloride test (Lakon 1949). The moisture content of the native grains was found to be 8.41±0.45%, following which the grains were stored in polythene bags at 4 ^{o}C until further use. The chemicals used for analysis were procured from Sigma-Aldrich Chemical Co., (St. Louis, Mo, USA).

Germination of foxtail millet grains

The foxtail millet grains were washed using 1.5% formaldehyde solution to prevent any contamination. To remove the traces formaldehyde, the grains were then washed thoroughly with distilled water and tested for any residues using the ferric chloride method described by VICH Steering Committee (2002). Prior to germination, the foxtail millet grains were first soaked in deionised water for 15h and then were subjected to germination in a controlled-environment growth cabinet. The temperature was maintained at 25±2 ^{o}C and the relative humidity was controlled at 50%; these conditions were based on the work reported by Sharma et al. (2015). Following the method described by Elkhalifa and Bernhardt (2010), the activities of alpha amylase and protease were monitored at regular intervals of 12 hours, and

the germination period of 72h represented the time taken for their activities to reach a maximum value., as. The maximum alpha amylase and protease activity was found to be attained after 72h (Fig. 1). The germinated foxtail millet grains were dried to a final moisture content of 7 – 8%, packed and stored in air-tight containers at 4 ^{o}C until further analysis. Non-germinated foxtail millet grains were used as a control.

High pressure soaking

Both germinated and non-germinated foxtail millet grains (25g each) were subjected to high hydrostatic pressures in a temperature-controlled pressure vessel system (vessel dimensions: 37mm diameter and 246mm length, Food LAB 900, Stansted Fluid Power Ltd., Stansted, UK). A blend of castor oil and ethanol in a ratio of 80:20 v/v was used as a medium to transmit pressure to the packed samples in the pressure vessel chamber. The foxtail millet grains were treated at a pressure of 400 MPa for 60 mins at a temperature of 60 ^{o}C. For this, 25g foxtail millet grain samples were suspended in 150ml of deionised water and sealed with virtually no headspace polyethylene pouches of dimensions 3cm × 20cm by employing Cryovac^{TM}. All the experiments were triplicated.

After high-pressure processing under specified conditions of pressure and temperature for a stipulated time, the water was completely drained from the pouches and the water occluding to the grains separated, was then blotted using a tissue paper. The processed grains were then subjected to freeze drying and were finally milled into fine flour passing through sieves of mesh sizes ranging between 100 and 200µm, using vibratory sieve shaker (Fritsch Analysette 3, Germany). The resulting flour was packed and stored in air-tight containers at 4 ^{o}C until further analysis.

Determination of functional properties

The bulk density, porosity and flowability of the optimized foxtail millet flour, as the angle of repose (as a static measure for flowability), were determined by the method of Sjollema (1963). The occluded air content was determined by the methods used by Jha et al. (2002). The wettability was determined by the method given by Muers and House (1962). The dispersibility of the optimized baby food was determined by the method described by the American Dry Milk Institute (ADMI 1965). The insolubility index was determined by the modified ADMI method described by Jha et al. (2002). The water, oil absorption capacity and swelling capacity of the product were determined by the method described by Sodipo and

Fashakin (2011). The emulsion activity, emulsion stability, foaming capacity and foaming stability were determined using the methods described by Elkhalifa and Benhardt (2010).

Finally, the gelatinization temperatures were determined using Differential Scanning Calorimetry, where a suspension of the resulting flour in deionised water was prepared in a ratio of 1:3; equilibrated for 15-18 h at ambient temperature; and presented to the differential scanning calorimeter, equipped with a built-in software (Model Q 2000a TA Instruments, New Castle, U.S.A.). A 10-12 mg suspension sample was weighed precisely in an aluminium sample pan and hermetically sealed. A similar empty pan was used as a reference for the analysis. A temperature range of 10 to 140 ^{o}C was used for scanning the sample in the pan at a heating rate of 10 ^{o}C min^{-1}. The resulting thermogram gave the values of onset (T_o), peak (T_p) and conclusion temperatures (T_c) in ^{o}C.

Sorption studies

Gravimetric method described by Lang et al. (1981), was used to determine the sorption isotherms for processed foxtail millet flour. The saturated salt solutions of eight reagent-grade salts, namely, lithium chloride, magnesium chloride, potassium carbonate, magnesium nitrate, sodium chloride, potassium chloride, potassium nitrate, and potassium sulfate, were chosen as mentioned by Greenspan (1977) to cover the water activity range from 0.11 to 0.97. It is important to note that the water activity values for these salts can show slight variations at different temperatures. Therefore, different water activity values of these salts at temperatures 10, 25 and 40 ^{o}C were used in this study. These saturated solutions were placed in air tight, wide mouth glass jars. Approximately 1 g of sample was weighed into a glass beaker placed on glass bead support inside the glass jar. The glass beakers were equilibrated for three days with the humid atmosphere before placing the sample. Then the moisture sorption characteristics were studied at 10, 25 and 40 ^{o}C (± 2 °C) by placing the sample containing glass jars in incubators for equilibration. These conditions were chosen in this study, as they represent the possible storage conditions for cereals like rice (Ondier et al. 2012) The samples in bottles were weighed at a regular interval of 3 days till a constant weight was attained. Equilibrium was considered to have accomplished when the weight difference between two successive weighing was less than 1 mg. Experiment was conducted in triplicates for all the samples at each relative humidity and temperature conditions. After the equilibrium has been attained, the moisture content of the samples was determined and was expressed in gram per litre (g/L). The average standard deviation between the replicates was calculated to be less

than 1% of the mean of the three values. These average values of equilibrium moisture content were then plotted against relative humidities or water activities to obtain moisture sorption isotherms.

Sorption model

Various approaches have been used to describe sorption isotherms of foods. Amongst which, Guggenheim-Anderson-De Boer (GAB) (Pérez-Alonso et al. 2006) is mostly used to study the correlation between the equilibrium moisture content (M) and water activity (a_w) for various foods. The following linearized form of GAB model were used for evaluating the best fitted values of model constants using linear regression:

GAB

$$W = W_o \frac{Gka_w}{(1-ka_w)(1-ka_w+Gka_w)} \quad (1)$$

The GAB model could be rearranged into a second-degree polynomial equation as given below:

$$\frac{a_w}{W} = aa_w^2 + ba_w + c \quad (2)$$

where, a, b and c are model constants and significantly depend on type of regression analysis. A nonlinear regression analysis of a_w/W v/s a_w yields a polynomial equation of the second order. The coefficients a, b and c were thus obtained from this polynomial equation and then substituted to obtain GAB constants W_o, G and k. W_o is the moisture content corresponding to saturation of all primary adsorption sites by one water molecule, G is the Guggenheim constant and k is the factor correcting for properties of multilayer molecule with respect to the bulk liquid.

Thermodynamic properties

The integral enthalpy, also known as, net isosteric heat of sorption was determined using Clausius-Clayperon equation (Rizvi 1986; Bell and Labuza 2000):

$$\frac{\partial(lna_w)}{\partial(\frac{1}{T})} = \frac{Q_{st}}{R} \quad (3)$$

where, T is the absolute temperature (K), Q_{st} is the net isosteric heat of sorption (kJ mol^{-1}) and R is the universal gas constant (8.314 × 10^{-3} kJ mol^{-1} K^{-1}).

The calculation procedure assumed that net heat of sorption was independent of temperature change. The slope of the plot of ln (a_w) versus *1/T* at constant moisture content gave the net isosteric heat of sorption (Eq. 3). Adding the latent heat of vaporization of pure water at 10, 25 and 40 ºC to the net isosteric heat of sorption (Q_{st}), gave the values of isosteric heat of sorption. A cubic spline interpolation was used to determine a_w values at various temperatures for a given moisture content (M).

Substituting free Gibbs energy in the Gibbs- Helmholtz equation (McMinn and Magee 2003; Kaya and Kahyaoglu 2005), the differential entropy was calculated using the following equation:

$$-\ln(a_w) = \frac{-(Q_{st}+\lambda)}{RT} - \frac{\Delta S}{R} \quad (4)$$

where, λ is the latent heat of vaporization of pure water (44.045 kJ mol^{-1} at 25 °C), and ΔS is the integral entropy of sorption (kJ mol^{-1} K^{-1}). The maximum storage stability point is when the water activity and temperature gives the minimum value of integral entropy (Alpizar-Reyes et al. 2017).

From the intercept of the plot of ln (a_w) versus *1/T* at specified moisture levels of eq. (4), the integral entropy was evaluated.

Isokinetic theory

A linear relationship between the isosteric heat of sorption (differential enthalpy) and differential entropy established the enthalpy- entropy theory (McMinn and Magee et al. 2003; Arslan and Togrul 2006):

$$Q_{st} = T_\beta \Delta S_d + \alpha \quad (5)$$

where, Q_{st} is the isosteric heat of sorption (kJ mol^{-1}), T_β is the isokinetic temperature (K), and α is the constant or Gibb's free energy (kJ mol^{-1}).

The isokinetic temperature (T_β) is a characteristic property of the material surface (Aguerre et al. 1986), and it represents the slope of the enthalpy- entropy linear relationship (Eq. 5).

Linear regression of Q_{st} with ΔS_d evaluated T_β. A statistical test proposed by Krug et al. (1976) verified the enthalpy- entropy compensation theory by defining the harmonic mean temperature (T_{hm}) as:

$$T_{hm} = \frac{n}{\sum_1^n (\frac{1}{T})} \quad (6)$$

where, T_{hm} is the harmonic mean temperature (K), and n is the number of temperature levels. Linear enthalpy- entropy compensation theory applies only when $T_\beta \neq T_{hm}$; the process is enthalpy driven if $T_\beta > T_{hm}$ and entropy driven if $T_\beta < T_{hm}$ (Leffler and Grunwald 1963). Eq. (6) shows that T_{hm} is a function of temperature levels selected for the experiment and is independent of the material considered. Analyses were conducted with $\alpha = 0$ to evaluate the effect of temperature on the sorption behaviour by introducing a temperature correction factor (Aguerre et al. 1986) as:

$$-\ln(a_w) = \frac{Q_{st}}{R(\frac{1}{T}-\frac{1}{T_\beta})^{-1}} \quad (7)$$

Spreading pressures

Spreading pressure was evaluated based on the analytical procedure described by Iglesias et al. (1976) and Fasina et al. (1999). Spreading pressure is given by the following equation:

$$\pi = \frac{KT}{A_m}\int_0^{a_w} \frac{x}{x_m a_w} \quad (8)$$

where, π is the spreading pressure (J m^{-2}), K is the Boltzman constant (1.380×10^{-23} J K^{-1}) and A_m is the surface area of a water molecule (1.06×10^{-19} m^2).

This integral becomes indeterminate at $a_w = 0.0$. Therefore, spreading pressure was evaluated by dividing the total limit (0.0 to a_w) into a very small interval of 0.0 to 0.05 and the remaining 0.05 to a_w. The integral in the first infinitesimal a_w range (0.0 to 0.05) was evaluated assuming a linear relationship (Henry's law) between m and a_w with usual notations (Fasina et al. 1999) as:

$$\pi = \frac{KTx}{A_m x_m} \quad (9)$$

The integral in the second a_w range (0.05 to a_w) was evaluated after fitting isotherm data (m, a_w) to the GAB model equation and the spreading pressure was obtained by integrating the equation in the second interval of 0.05 to a_w (Iglesias et al. 1976):

$$\pi = \frac{KT}{A_m} ln \left[\frac{1+Cka_w-ka_w}{1-ka_w}\right]_{0.05}^{a_w} \quad (10)$$

Adding the results of the two selected a_w intervals produced the spreading pressures at any studied temperature and water activity combination.

Glass transition temperature

Differential scanning calorimetry was used to determine the glass transition temperature. A suspension of processed foxtail millet flours and deionised water was prepared in a ratio of 1:3 and equilibrated for 15-18 h at ambient temperatures and were analysed using a TA Instruments model Q-2000 differential scanning calorimeter, equipped with a built-in software (TA Instruments, Newcastle, U.S.A.). For this, 10-12 mg of flour, equilibrated at a range of water activities (0.11 – 0.85) and temperatures (10, 25 and 40 ^oC) were weighed in an aluminium sample pan and hermetically sealed. A similar empty pan was used as a reference for the analysis. A temperature range of -50 to 150 ^oC was used for scanning the sample in the pan with a heating rate of 2 ^oC min^{-1} (Alpizar-Reyes et al. 2017). The resulting thermogram gave the values of onset (T_o), peak (T_p) and conclusion temperatures (T_c) in ^oC and gelatinisation enthalpies (ΔH) in kJ kg^{-1}. The final values obtained were an average of three replicates for each sample, with a maximum deviation of less than 1.5%. The midpoint of the baseline shift obtained using DSC was taken as the glass transition temperature (T_g). The measurements were made in triplicates. Further, to deduce the plasticizing effect of water on T_g, the DSC data was put in the Gordon-Taylor equation:

$$T_g = \frac{W_1 T_{g1} + KW_2 T_{g2}}{W_1 + KW_2} \quad (11)$$

Where, W_1 and W_2 are the mass fractions of the flours and of water, respectively, T_{g1} is the T_g value of flour at zero moisture content and T_{g2} is the T_g value of water (-135 ^oC), and K is a constant.

Statistical analysis

The differences amongst the samples were determined using one-way analysis of variance (ANOVA) using Minitab 17.0 software. Using the Duncan's test the differences were considered statistically significant at p-value ≤ 0.05. The degree of fitness of the model was evaluated using determination coefficient (R^2).

Results and discussion

Functional properties of the flours

The functional properties of the processed germinated foxtail millet flour (GFMF) as well as non-germinated foxtail millet flour (NGFMF) are shown in Table 1. Germination of foxtail millet increased the values of porosity, occluded air content, water and oil absorption capacity, dispersibility, swelling capacity, wettability, flowability, gelatinization enthalpy, emulsification activity and stability; while decreased the values of bulk density, insolubility index, foaming capacity and stability. Albarracín et al. (2016) reported that the water absorption and water solubility values were higher for germinated brown rice samples as compared to the control brown rice samples. Similar results were also stated by Chinma et al. (2009) for varieties of germinated tigernut flour; Devisetti et al. (2014) for millet flours and Elkhalifa and Bernhardt (2010) for germinated sorghum flour.

Moisture sorption characteristics

The effect of germination was studied for the stability of the high pressure processed foxtail millet flours.

Equilibrium moisture content- water activity

The relationship between the EMC and water activity (a_w) at a constant temperature forms the MSI. Therefore, foods with different moisture content have different water activity, thus they form their own sorption isotherm (Alpizar-Reyes et al. 2017). Fig. 2 (a, b) shows the experimental isotherms for NGFMF and GFMF at 10, 25 and 40 ^{o}C, respectively, with which the thermodynamic functions related to moisture sorption in porridge flours were determined. Both figures depict that the EMC increased with increasing water activity ranging from 0.11 to 0.97 at a constant temperature. A constant linear increase in EMC at lower water activities ranging from 0.11 to 0.55 was observed for NGFMF and from 0.11 to 0.76 for GFMF, which

could be due to the ability of the flour to lower the vapour pressure, with the decrease in the relative humidity. While, a rapid increase in EMC at higher water activities from 0.55 to 0.97 for NGFMF (Fig. 2(a)) and an impulsive increase (Fig. 2(b)) in the EMC from 0.76 to 0.97 for GFPF could be attributed to the high sorptive capacity of hydrophilic starch in foxtail millet flours consisting of a large number of free hydroxyl sites (Pollatos et al. 2013). This impulsive increase in the case of GFMF could be because of elevated enzyme activity and breakdown of complex sugars into simple sugars during germination (Wu et al. 2013). Barreiro et al. (2003) also found similar results for malted barley flours. Therefore, it could be concluded from the results that GFMF would require improved storage conditions with relative humidity not exceeding 76% and NGFMF not exceeding 55%.

The increase in temperatures did not have a significant effect on the moisture sorption behaviour of both the flours. Though it was observed that for NGFMF, the EMC decreased with the increase in temperatures for a given water activity, showing a less hygroscopic behaviour of NGFMF at higher temperatures. This is because high temperatures increase the kinetic energy of the water molecules, thus increasing the distance between them and causing easy binding of these water molecules to the suface of the flours (Pollatos et al. 2013; Alpizar-Reyes et al. 2017). On the other hand, an opposite trend was depicted by GFMF, which could be attributed to the higher content of sugars due to germination, thus increasing the active sites for the sorption of water by proteins (Barreiro et al. 2003; Pollatos et al. 2013). In addition to this, the MSI's of both NGFMF and GFMF were of the characteristic sigmoidal shape (BET II type), which is likely found in all types of dry foods rich in starch and sugars.

Sorption models

The experimental sorption data for both the flours were fitted using GAB model, with R^2 value of more than 0.998 at all temperatures and RMSE value of less than 0.051. The model parameters were determined using non-linear regression method. Table 2 and 3 shows the model parameters for NGFMF and GFMF, respectively. MSIs of both the flours can be divided into an: (1) initial monolayer region (a_w less than 0.2), where the water molecules are strongly absorbed as critical moisture content that starts the chemical reactions in foods. It is also a measure of the availability of active sorption sites; (2) an intermediate multilayer region (a_w in the range of 0.2-0.6), that causes lipid oxidation and physical changes in foods, and (3) a final condensed water region (a_w greater than 0.6), which ascertains the microbial

growth (Labuza and Altunakar 2007). The values of monolayer moisture content (W_o) for both NGFMF and GFMF decreased with the increase in temperatures from 10 to 40 ^oC, as expected by the theory of physical sorption (Pollatos et al. 2013). The values for W_o for NGFMF and GFMF ranged between 3.235 - 2.364 g g^{-1} and 2.987 – 2.063 g g^{-1}, respectively. The composition and nature of the product was responsible for the difference in the values of the monolayer moisture content in germinated and non-germinated flours. Thus, NGFMF being a starch rich flour was found to be more hygroscopic and GFMF being a sugar rich flour due to germination, was found to be less hygroscopic.

The constant *G* is related to the monolayer sorption heat which associates the chemical potential difference with the superior layers of moisture in the flour structure. It has been established that low temperatures assist the formation of strong adsorbent and adsorbate interactions, thus causing an increase in the *G* values with the increase in temperature (Alpizar-Reyes et al. 2017). While, this study reported a decrease in the *G* values on increasing the temperature from 10 to 25 ^oC and then an increase in the *G* values on further increasing the temperature from 25 to 40 ^oC, for both NGFMF and GFMF. Thus, it suggested that the flour-water interactions in both NGFMF and GFMF decreased as follows: 10 ^oC > 40 ^oC > 25 ^oC. These results agreed with Pollatos et al. (2013) and Simha et al. (2016).

Another constant *k* is related to the enthalpy of water multilayer sorption indicating a measure of the interactions between multilayer molecules and adsorbent. When, *k* values are in the range of 0.24 to 1.0, GAB model best describes the sigmoid shaped isotherms (Lewicki 1997). For NGFMF and GFMF, the *k* values were in the range of 0.780 – 0.881 and 0.852 – 0.944, respectively. Since the values $k << 1$, so it was inferred that the flours comprised of a structured state of adsorbate in the adjacent layers to the monolyer (Alpizar-Reyes et al. 2017).

Thermodynamic properties

Dried foods like the flours that have been studied here, undergo various changes during storage due to the processes like crystallization, dissolution, diffusion, swelling, etc. Therefore, various thermodynamic properties like integral enthalpy and entropy determines the condition of maximum food stability.

352 Net isosteric heat of sorption

353 The degree of bound water in the flour estimates the variation in the integral enthalpy which
354 is also known as net isosteric heat of sorption (Q_{st}). It indicates the interaction of water
355 vapour with solid substrates in the flours, thus explaining the endothermic or exothermic
356 nature of the interaction (Pushpadass et al. 2014). Fig. 3 (a, b) shows the relationship between
357 Q_{st} and the moisture content at constant temperature for both NGFMF and GFMF. The
358 negative values of Q_{st} in the graph indicated the exothermic nature of sorption for both flours.
359 Strong water-substrate interactions were suggested at low moisture contents, as the water
360 binding capacity of the flours increased with the increase in the negative values of Q_{st}. The
361 values of Q_{st} ranged between -76.35 kJ mol^{-1} to -38.23 kJ mol^{-1} for NGFMF and 172.55 kJ
362 mol^{-1} to -34.02 kJ mol^{-1} for GFMF at a moisture range of 0 to 36%. At the higher moisture
363 contents, the value of Q_{st} became close to the values of heat of sorption of pure water, thus
364 indicating the excess moisture bounded to the flours or condensation in the capillaries of flour
365 particulates. The difference in the Q_{st} of both flours at low moisture contents indicated that
366 the degree of binding of water molecules was higher for GFMF as compared to the NGFMF.
367 This could be because of the availability of the higher energy polar sites on the surface in the
368 initial stages of sorption of GFMF, causing water molecules to form a monomolecular layer.
369 In addition to this, as the moisture content further increased for both the flours, the
370 availability of these sites decreased and sorption occurred at less active sites, yielding lower
371 heats of sorption (Lagoudaki and Demertzis 1994). Similar findings were observed for
372 chestnut and wheat flours (Moreira et al. 2010); Japanese durum wheat flour (Chuma et al.
373 2012); whole wheat flour (Martín- Santos et al. 2012) and Greek durum wheat semolina
374 (Pollatos et al. 2013).

375 Integral entropy

376 The integral entropy of sorption (ΔS) for NGFMF ranged between -0.404 to -0.120
377 kJ mol^{-1} K^{-1}, with a minimum value at 4% moisture content and 40 ^{o}C temperature and for
378 GFMF between -0.667 to -0.383 kJ mol^{-1} K^{-1}, with a minimum value at 8% moisture content
379 and 10 ^{o}C temperature. Fig. 4 (a, b) shows the integral entropy as a function of moisture
380 content at 10, 25 and 40 ^{o}C for both flours. These findings were in accordance with Simha et
381 al. (2016). The minimum ΔS value was observed for GFMF as compared to NGFMF, thus
382 interpreting that GFMF is more stable than NGFMF at a temperature range of 10 to 40 ^{o}C.
383 This stability is because the water molecules in the flour forms more ordered arrangement,

bond between adsorbate and adsorbent being the strongest. Therefore, less moisture is available for spoilage reactions. The subsequent increase in the values of ΔS with the increase in moisture content for both the flours, reflected the formation of multi-layers and freely held molecules of water (Rizvi 1986). The increasing temperatures also had a great impact on the integral entropy of both the flours. With the increase in temperature from 10 to 40 ^{o}C, the values of ΔS decreased for NGFMF and increased for GFMF, suggesting that NGFMF was more stable at higher temperatures, while GFMF was more stable at lower temperatures. This could be attributed to the composition of the flours.

Enthalpy-entropy compensation theory

The isokinetic theory or the enthalpy-entropy compensation theory determines the existence of true compensation by comparing the difference between the harmonic temperature (T_{hm}) and isokinetic temperature (T_{β}) ($T_{hm} \neq T_{\beta}$). This theory helps in evaluating the sorption reactions, confirming if the reactions are enthalpy driven or entropy driven. According to Leffler and Grunwald (1963), if $T_{\beta} > T_{hm}$ the process is enthalpy driven, while if $T_{\beta} < T_{hm}$ the process is considered to be entropy controlled. The T_{hm} values were found to be 297 K and 303 K at all three temperatures for NGFMF and GFMF, respectively. The results of this study showed that the T_{β} values were greater than T_{hm} at all three temperatures, therefore it was concluded that the sorption reactions for both NGFMF and GFMF were enthalpy-controlled processes in the studied moisture content range. This further confirmed the predominance of mesopores in the interactions between water-flour (Azuara and Beristain 2006). These values were calculated by fitting the data in Eq. 7. Fig. 5 (a, b) depicts the enthalpy-entropy compensation obtained by plotting the integral properties of both flours at constant temperatures of 10, 25 and 40 ^{o}C. The linear relationship between the two thermodynamic properties confirmed the existence of compensation theory, which has been already justified for various foods by Fontan et al. (1982).

Spreading pressures

The spreading pressures (π) represents the excess of free energy at the surface of the flours, and provides an indication of the increase in surface tension at free sorption sites due to adsorbed molecules (Fasina et al. 1999). The spreading pressure isotherms for both NGFMF and GFMF were plotted against the water activity at 10, 25 and 40 ^{o}C (Fig. 6 (a, b)). The values of π lied in the range of 0 – 0.078 J m^{-2} for NGFMF and 0 – 0.124 J m^{-2} for GFMF,

indicating higher surface tension on the surface of GFMF at high water activities. The graph showed that the value of π increased with increasing water activity and decreased with increasing temperatures. While, at water activities above 0.76 the values of π significantly increased with increasing temperatures. Similar trend was observed for cassava flour (Ayala-Aponte 2016) and milk-foxtail millet powder (Simha et al. 2016).

Glass transition temperatures

DSC thermograms obtained for both NGFMF and GFMF at a range of water activities between 0.11 to 0.97 at 10, 25 and 40 ^{o}C, gave the values of glass transition temperatures (T_g). T_g was obtained from the midpoint of the typical heat capacity change in the thermogram line over a range of temperatures (Sandoval et al. 2009). Increasing temperatures did not have any significant effect on the T_g values of both flours. Fig. 7 (a, b) shows the relationship between T_g and water activity at constant temperature. It was observed that as the water activity increased the values of T_g decreased linearly for both the flours, ranging between 82.25 to 28.67 ^{o}C for NGFMF and from 51.11 to 11.83 ^{o}C for GFMF at all three temperatures. The lower values of GFMF could be attributed to the conversion of starch into sugars and other compounds due to germination of foxtail millet flours. The low molecular weight of sugars and other compounds formed of germination, have been reported to cause plasticizing effect of small molecules on starchy products (Chen and Yeh 2000). While, the decrease in T_g values with increasing temperatures and water activities could be explained by the plasticizing effect of water. Increasing temperatures causes decrease in the attractive forces, thereby causing slow motion of water molecules, that gets easily adsorbed on the flour surfaces, thus decreasing the T_g values. Whereas, increasing water activities, increases the moisture content in the flours that acts as plasticizers, thus changing the glassy material into rubbery state (Alpizar-Reyes et al. 2017).

The experimental values of T_g for NGFMF and GFMF stored at different water activities and temperatures were fitted in Eq. 3.8.12 with a R^2 value of 0.991. The estimated values of T_g were found to be 124.36 ^{o}C for NGFMF and 101.82 ^{o}C for GFMF. This difference in the result could be due to erratic decrease in the experimental T_g values with increasing water activity, predominantly in NGFMF as compared to GFMF. Similar justification was provided for lower T_g values of dry amorphous materials in comparison to pure starch materials by Sandoval et al. (2009).

Conclusion

The germinated and non-germinated flours obtained from high pressure processed foxtail millet grains were studied for their moisture sorption characteristics to understand the interdependence between the water and the foxtail millet grain components. Thus, the moisture sorption isotherms provided information regarding the stability of these flours in any environment. Apart from this, the thermodynamic properties were also studied that gave information on the changes that took place in the flours during storage. Sorption moisture isotherms showed a sigmoidal type II shape. Experimental data for these isotherms at 10, 25 and 40 °C fitted satisfactorily to the GAB model. Sorption properties of processed germinated and non-germinated foxtail millet flour indicated that the percent of bound water decreased for NGFPF and increased for GFPF, as the temperature increased, confirming that the availability of active sites decreased due to a reduction in the total sorption ability for NGFPF and vice-versa for GFPF. This work also suggested that the moisture sorption, thermodynamic properties, spreading pressures and glass transition temperatures can be related to obtain conditions guaranteeing maximum stability for storage of the flours.

Acknowledgement Nitya Sharma gratefully acknowledges the support provided by the Commonwealth Scholarship Commission (INCN-2015-124).

References

Abebe, W., & Ronda, F. (2015) Flowability, moisture sorption and thermal properties of tef [*Eragrostis tef* (Zucc.) Trotter] grain flours. *Journal of Cereal Science, 63*, 14-20.

ADMI (1965). Standards for grades of dry milk including methods of analysis. *American Dry Milk Institute Bulletin*, USA.

Aguerre, R. J., Suarez, C., & Viollaz, P. E. (1986) Enthalpy- entropy compensation in sorption phenomena: Application to the prediction of the effect of temperature on food isotherms. *Journal of Food Science*. *51*(6),1547-1549.

Al-Mahasneh, M., Alkoaik, F., Khalil, A., Al-Mahasneh, A., El-Waziry, A., Fulleros, R., & Rababah, T. (2014) A generic method for determining moisture sorption isotherms of cereal grains and legumes using artificial neural networks. *Journal of Food Process Engineering*, *37*, 308-316.

475 Albarracín, M., Talens, P., Martínez-Navarrete, N., González, R. J., & Drago, S. R. (2016)
476 Physicochemical properties and structural characteristics of whole grain *Oryza*
477 *sativa* L. with different treatments. *Food Science and Technology*
478 *International*, *22*(4), 333-342.

479 Alpizar-Reyes, E., Carrillo-Navas, H., Romero-Romero, R., Varela-Guerrero, V., Alvarez-
480 Ramírez, J., & Pérez-Alonso, C. (2017) Thermodynamic sorption properties and
481 glass transition temperature of tamarind seed mucilage (*Tamarindus indica* L.).
482 *Food and Bioproducts Processing*. *101*, 166-176.

483 Arslan, N., & Togrul, H. (2006) The fitting of various models to water sorption isotherms of
484 tea stored in a chamber under controlled temperature and humidity. *Journal of*
485 *Stored Products Research*, *42*(2), 112- 135.

486 Ayala-Aponte, A. A. (2016) Thermodynamic properties of moisture sorption in cassava
487 flour. *Dyna*, *83*(197), 138-144.

488 Azuara, E., & Beristain, C. I. (2006) Enthalpic and entropic mechanisms related to water
489 sorption of yogurt. *Drying Technology*, *24*(11), 1501-1507.

490 Barreiro, J. A., Fernández, S., & Sandoval, A. J. (2003) Water sorption characteristics of six
491 row barley malt (*Hordeum vulgare*). *LWT-Food Science and Technology*, *36*(1),
492 37-42.

493 Bell, L. N., & Labuza, T. P. (2000) Moisture Sorption: Practical Aspects of Isotherm
494 Measurement and Use. St. Paul, Minnesota, USA: *American Association of Cereal*
495 *Chemists*.

496 Brett, B., Figueroa, M., Sandoval, A. J., Barreiro, J. A., & Müller, A. J. (2009) Moisture
497 sorption characteristics of starchy products: oat flour and rice flour. *Food*
498 *Biophysics*, *4*(3), 151-157.

499 Chen, C. M., & Yeh, A. I. (2000) Expansion of rice pellets: Examination of glass transition
500 and expansion temperature. *Journal of Cereal Science*, *32*(2), 137–145.

501 Chinma, C. E., Adewuyi, O., & Abu, J. O. (2009) Effect of germination on the chemical,
502 functional and pasting properties of flour from brown and yellow varieties of
503 tigernut (*Cyperus esculentus*). *Food Research International*, *42*(8), 1004-1009.

504 Chuma, A., Ogawa, T., Kobayashi, T., & Adachi, S. (2012) Moisture sorption isotherm of
505 durum wheat flour. *Food Science and Technology Research*, *18*(5), 617-622.

506 Devisetti, R., Yadahally, S. N., & Bhattacharya, S. (2014) Nutrients and antinutrients in
507 foxtail and proso millet milled fractions: Evaluation of their flour
508 functionality. *LWT-Food Science and Technology*, *59*(2), 889-895.

509 Elkhalifa, A. E. O., & Bernhardt, R. (2010) Influence of grain germination on functional
510 properties of sorghum flour. *Food Chemistry*, *121*(2), 387-392.

511 Erbaş, M., Aykin, E., Arslan, S., & Durak, A. N. (2016) Adsorption behaviour of bulgur.
512 *Food Chemistry*, *195*, 87-90.

513 Estrada-Girón, Y., Swanson, B. G., & Barbosa-Cánovas, G. V. (2005) Advances in the use of
514 high hydrostatic pressure for processing cereal grains and legumes. *Trends in Food*
515 *Science and Technology*, *16*, 194-203.

516 Fasina, O. O., Ajibola, O. O., & Tyler, R. T. (1999) Thermodynamics of moisture sorption in
517 winged bean seed and gari. *Journal of Food Process Engineering*, *22*(6), 405-418.

518 Fasina, O., Sokhansanj, S., & Tyler, R. (1997) Thermodynamics of moisture sorption in
519 alfalfa pellets. *Drying Technology*, *15*(5), 1553-1570.

520 Fontan, C. F., Chirife, J., Sancho, E., & Iglesias, H. A. (1982) Analysis of a model for water
521 sorption phenomena in foods. *Journal of Food Science*, *47*(5), 1590-1594.

522 Greenspan, L. (1977) Humidity fixed points of binary saturated aqueous solutions. *Journal of*
523 *Research of the National Bureau of Standards*, *81*(1), 89-96.

524 Iglesias, H. A., Chirife, J., & Viollaz, P. (1976) Thermodynamics of water vapour sorption by
525 sugar beet root. *Journal of Food Technology*, *11*(1), 91- 101.

526 Ikhu- Omoregbe, D. I. O., & Chen, X. D. (2005) Use of sorption isotherms for the estimation
527 of shelf life of two Zimbabwean flours. *Developments in Chemical Engineering*
528 *and Mineral Processing*, *13*(1- 2), 79-90.

529 Jha, A., Patel, A. A., & Singh, R. R. B. (2002) Physico-chemical properties of instant *kheer*
530 mix. *Le Lait*, *82*(4), 501-513.

531 Katz, E. E., & Labuza, T. P. (1981) Effect of water activity on the sensory crispness and
532 mechanical deformation of snack food products. *Journal of Food Science*, *46*(2),
533 403-409.

534 Kaya, S., & Kahyaoglu, T. (2005) Thermodynamic properties and sorption equilibrium of
535 pestil (grape leather). *Journal of Food Engineering*, *71*(2), 200-207.

536 Krug, R. R., Hunter, W. G., & Grieger, R. A. (1976) Enthalpy-entropy compensation. 2.
537 Separation of the chemical from the statistical effect. *The Journal of Physical*
538 *Chemistry*, *80*(21), 2341-2351.

539 Labuza, T. P., Kaanane, A., & Chen, J. Y. (1985) Effect of temperature on the moisture
540 sorption isotherms and water activity shift of two dehydrated foods. *Journal of*
541 *Food Science*, *50*(2), 385-392.

542 Labuza, T. P., & Altunakar, B. (2007) Water activity prediction and moisture sorption
543 isotherms. *Water activity in foods: fundamentals and applications*, John Wiley &
544 Sons, *1*, 109-131.

545 Lagoudaki, M., & Demertzis, P. G. (1994) Equilibrium moisture characteristics of dehydrated
546 food constituents as studied by a modified inverse gas chromatographic
547 method. *Journal of the Science of Food and Agriculture*, *65*(1), 101-109.

548 Lagoudaki, M., Demertzis, P. G., & Kontominas, M. G. (1993) Moisture adsorption
549 behaviour of pasta products. *LWT-Food Science and Technology*, *26*(6), 512-516.

550 Lakon, G. (1949) The topographical tetrazolium method for determining the germinating
551 capacity of seeds. *Plant Physiology*, *24*(3), 389.

552 Lang, K. W., McCune, T. D., & Steinberg, M. P. (1981) A proximity equilibration cell for
553 rapid determination of sorption isotherms. *Journal of Food Science*, *46*(3), 936-
554 938.

555 Lasekan, O. O., & Lasekan, W. O. (2000) Moisture sorption and the degree of starch polymer
556 degradation on flours of popped and malted sorghum (*Sorghum bicolor*). *Journal*
557 *of cereal science*, *31*(1), 55-61.

558 Leffler, J. E., & Grunwald, E. (1963) *Rates and equilibria of organic reactions: as treated by*
559 *statistical, thermodynamic, and extrathermodynamic methods*. John Wiley & Sons,
560 Dover Publications, New York.

561 Lewicki, P. P. (1997) The applicability of the GAB model to food water sorption
562 isotherms. *International journal of food science & technology*, *32*(6), 553-557.

563 Martín- Santos, J., Vioque, M., & Gómez, R. (2012) Thermodynamic properties of moisture
564 adsorption of whole wheat flour. Calculation of net isosteric heat. *International*
565 *Journal of Food Science & Technology*, *47*(7), 1487-1495.

566 McMinn, W. A. M., & Magee, T. R. A. (2003) Thermodynamic properties of moisture
567 sorption of potato. *Journal of Food Engineering*, *60*(2), 157-165.

568 Moreira, R., Chenlo, F., Torres, M. D., & Prieto, D. M. (2010) Water adsorption and
569 desorption isotherms of chestnut and wheat flours. *Industrial crops and*
570 *products*, *32*(3), 252-257.

571 Muers, M. M., & House, T. U. (1962) A simple method for comparing wettability of instant
572 spray dried separated milk powder. In *Copenhagen, Denmark: XVI International*
573 *Dairy Congress*, *8*, 299.

574 Ondier, G. O., Siebenmorgen, T. J., & Mauromoustakos, A. (2012) Equilibrium moisture
575 contents of pureline, hybrid, and parboiled rice kernel fractions. *Applied*
576 *Engineering in Agriculture*, *28*(2), 237.

577 Pérez-Alonso, C., Beristain, C. I., Lobato-Calleros, C., Rodríguez-Huezo, M. E., & Vernon-
578 Carter, E. J. (2006) Thermodynamic analysis of the sorption isotherms of pure and
579 blended carbohydrate polymers. *Journal of Food Engineering*, *77*(4), 753-760.

580 Pollatos, E. P., Riganakos, K. A., & Demertzis, P. G. (2013) Moisture sorption characteristics
581 of Greek durum wheat semolina. *Starch - Stärke, 65*(11-12), 1051-1060.

582 Pushpadass, H. A., Emerald, F., Chaturvedi, B., & Rao, K. J. (2014) Moisture sorption
583 behavior and thermodynamic properties of *gulabjamun* mix. *Journal of Food*
584 *Processing and Preservation*, *38*(6), 2192-2200.

585 Rizvi, S. S. H. (1986) Thermodynamic properties of foods in dehydration. In: Rao MA, Rizvi
586 SSH, Datta AK (eds), *Engineering properties of food*, 3rd ed. CRC Press, Boca
587 Raton.

588 Rizvi, S. S. H., & Benado, A. L. (1983) Thermodynamic analysis of drying foods. *Drying*
589 *Technology*, *2*(4), 471-502.

590 Sandoval, A. J., Nuñez, M., Müller, A. J., Della Valle, G., & Lourdin, D. (2009) Glass
591 transition temperatures of a ready to eat breakfast cereal formulation and its main
592 components determined by DSC and DMTA. *Carbohydrate Polymers*, *76*(4), 528-
593 534.

594 Sharma, S., Saxena, D.C., & Riar, C.S. (2015) Antioxidant activity, total phenolics,
595 flavonoids and antinutritional characteristics of germinated foxtail millet (*Setaria*
596 *italica*). *Cogent Food & Agriculture, 1*(1), 1081728.

597 Sharma, N., & Niranjan, K. (2017) Foxtail millet: properties, processing, health benefits and
598 uses. *Food Reviews International*, DOI: 10.1080/87559129.2017.1290103.

599 Simha, H. V., Pushpadass, H. A., Franklin, M. E. E., Kumar, P. A., & Manimala, K. (2016)
600 Soft computing modelling of moisture sorption isotherms of milk-foxtail millet
601 powder and determination of thermodynamic properties. *Journal of food science*
602 *and technology*, *53*(6), 2705-2714.

603 Sjollema, A. (1963) Some investigations on the free-flowing properties and porosity of milk
604 powders. *Netherlands Milk and Dairy Journal*, *17*(3), 245-259.

605 Sodipo, M. A., & Fashakin, J. B. (2011) Physicochemical properties of a complementary diet
606 prepared from germinated maize, cowpea and pigeon
607 pea. *Journal of Food, Agriculture and Environment*, *9*(3-4), 23-25.

VICH Steering Committee (2002) Testing of residual formaldehyde. *VICH International Cooperation on Harmonization of Technical Registration of Veterinary Medical Products*, 4-6.

Wu, F., Chen, H., Yang, N., Wang, J., Duan, X., Jin, Z., & Xu, X. (2013) Effect of germination time on physicochemical properties of brown rice flour and starch from different rice cultivars. *Journal of Cereal Science*, *58*(2), 263-271.

Yu, Y., Ge, L., Ramaswamy, H. S., Wang, C., Zhan, Y., & Zhu, S. (2016) Effect of high-pressure processing on moisture sorption properties of brown rice. *Drying Technology*, *34*(7), 783-792.

Zhang, Q., Ge, L., Ramaswamy, H. S., Zhu, S., Yu, L., & Yu, Y. (2017) Modeling Equilibrium Moisture Content of Brown Rice as Affected by High-Pressure Processing. *Transactions of the ASABE*, *60*(2), 551-559.

Zhang, L., Li, J., Han, F., Ding, Z., & Fan, L. (2017) Effects of different processing methods on the antioxidant activity of 6 cultivars of foxtail millet. *Journal of Food Quality*, DOI: 10.1155/2017/8372854.

638 **TABLES**

639 **Table 1** Functional properties of processed foxtail millet flours

Property	GFMF	NGFMF
Bulk density (g l^{-1})	592±12.2^{b}	732±10.4^{a}
Porosity (% volume)	67.8±0.5^{a}	53.4±0.6^{b}
Occluded air content (ml 100ml^{-1})	105.3±2.0^{a}	94.6±1.8^{b}
Water absorption capacity (g 100g^{-1})	157.4±1.8^{a}	148.2±2.3^{b}
Oil absorption capacity (g 100g^{-1})	98.0±0.5^{a}	80.4±1.1^{b}
Dispersibility (%)	82.2±0.5^{a}	75.4±0.3^{b}
Insolubility index (ml)	3.1±0.2^{b}	4.7±0.1^{a}
Swelling capacity (ml g^{-1})	5.2±0.2^{a}	4.0±0.3^{b}
Wettability (s)	58.0±1.0^{a}	52.0±1.0^{b}
Flowability (θ)	70.1±0.4^{a}	62.3±0.9^{b}
Emulsion activity (%)	64.5±0.1^{a}	48.2±0.0^{b}
Emulsion stability (%)	82.4±0.2^{a}	66.5±0.1^{b}
Foaming capacity (%)	5.2±0.4^{b}	8.8±0.5^{a}
Foaming stability (%)	57.8±0.7^{b}	78.8±0.9^{a}
Gelatinization properties:		
1. Onset temperature (^{o}C)	70.05±0.92^{a}	70.05±1.03^{a}
2. Peak temperature (^{o}C)	73.16±1.11^{a}	73.01±1.13^{a}
3. Conclusion temperature (^{o}C)	77.25±0.88^{a}	77.13±0.98^{a}
4. Gelatinization enthalpy (J/g)	2.306±0.110^{a}	1.563±0.099^{b}

640 Values are mean of three replications (n=3) and expressed as mean ± standard deviation.
641 Means with different superscript within the same row are significantly different at $p \leq 0.05$.

642

643

644

645

646

Table 2 Estimated parameters of GAB sorption model for NGFMF

T (°C)	W_o (%)	G	k	R^2
10	3.235±0.100[a]	43.171±0.150[a]	0.780±0.020[a]	0.99
25	2.662±0.150[b]	28.260±0.200[b]	0.820±0.020[a]	0.99
40	2.364±0.090[b]	32.720±0.190[c]	0.881±0.025[a]	0.99

Values are mean of three replications (n=3) and expressed as mean ± standard deviation.

Table 3 Estimated parameters of GAB sorption model for GFMF

T (°C)	W_o (%)	G	k	R^2
10	2.987±0.090[a]	42.701±0.220[a]	0.852±0.025[a]	0.99
25	2.476±0.095[a]	28.912±0.150[b]	0.896±0.030[a]	0.98
40	2.063±0.090[a]	33.661±0.150[c]	0.944±0.010[a]	0.99

Values are mean of three replications (n=3) and expressed as mean ± standard deviation.

667 **FIGURES**

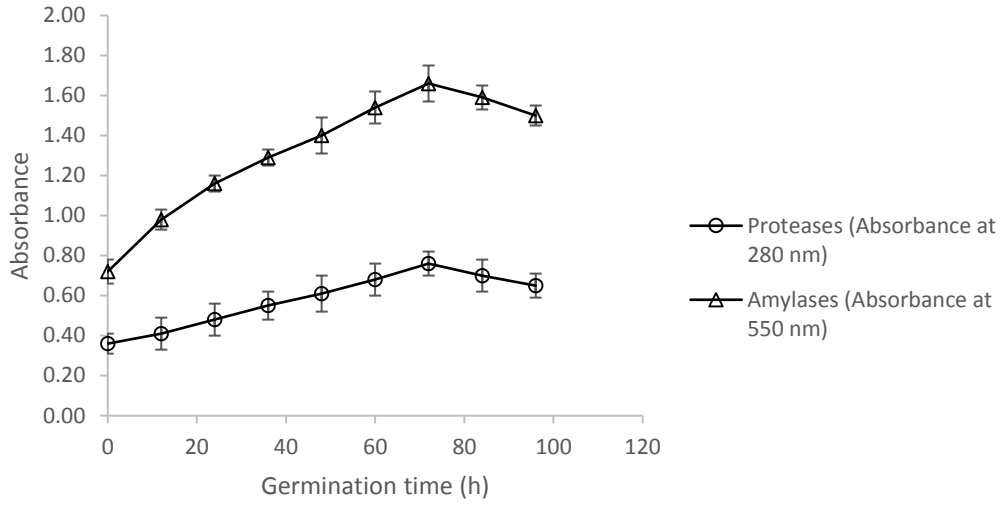

668

669 **Fig. 1** Protease and amylase activity variation during the germination of foxtail millet
670 grains (Temperature= 25±2 ^{o}C; RH=80%)

671

672

673

674

675

676

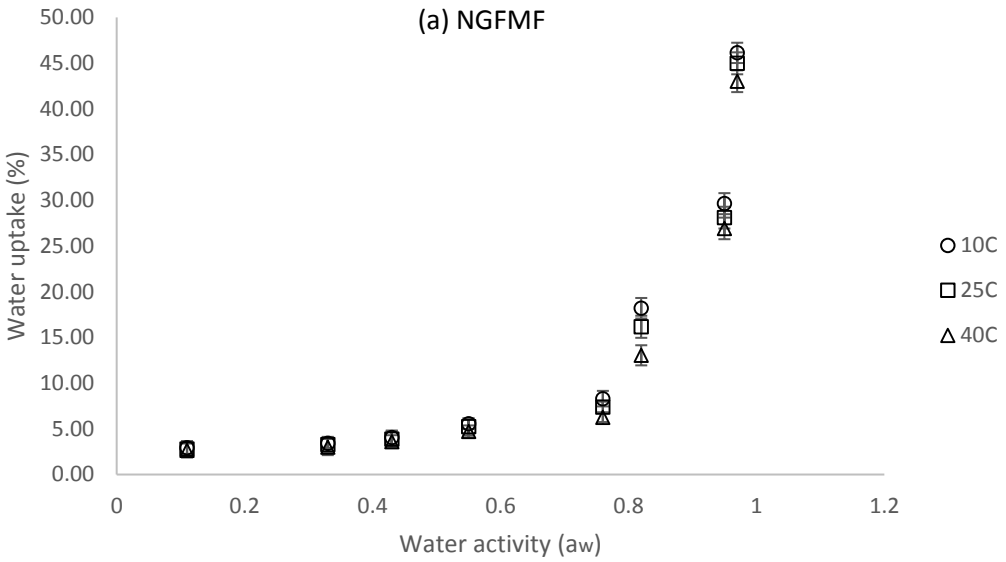

677

678

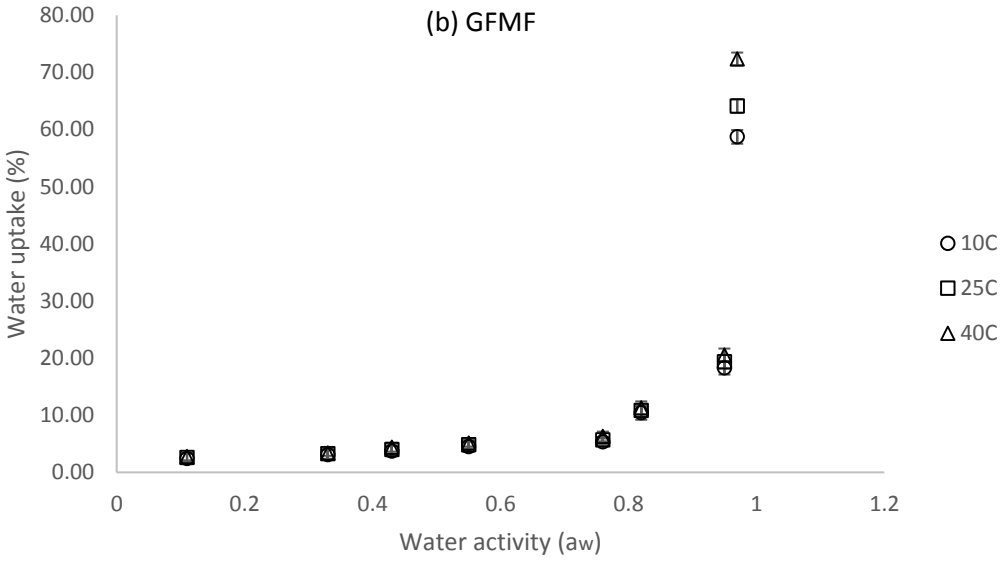

679

680 **Fig. 2** Moisture sorption isotherms for (a) NGFMF and (b) GFMF at 10, 25 and 40 ^{o}C
681 obtained by static gravimetric method

682

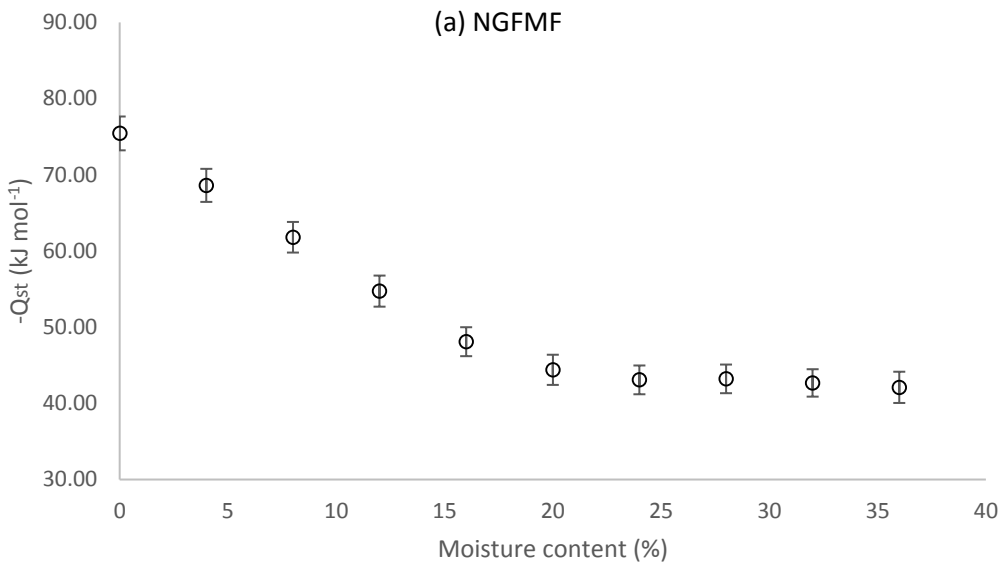

683

684

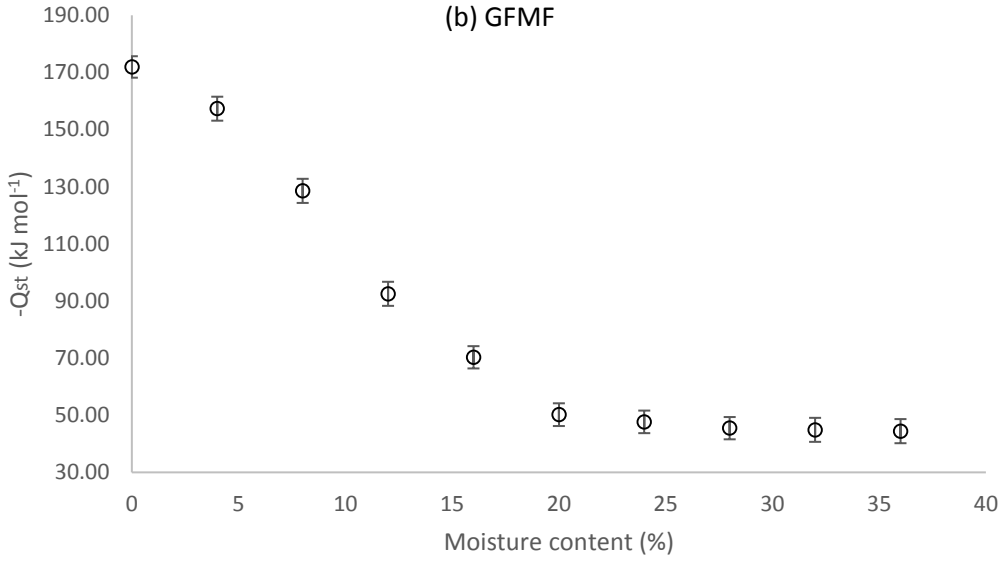

685

686 **Fig. 3** Net isosteric heat of sorption (Q_{st}) as a function of moisture content for (a)
687 NGFMF and (b) GFMF. The isoteric heat of sorption at any temperature can be
688 obtained by adding the latent heat at that temperature to the Qst values.

689

690

691

692

693

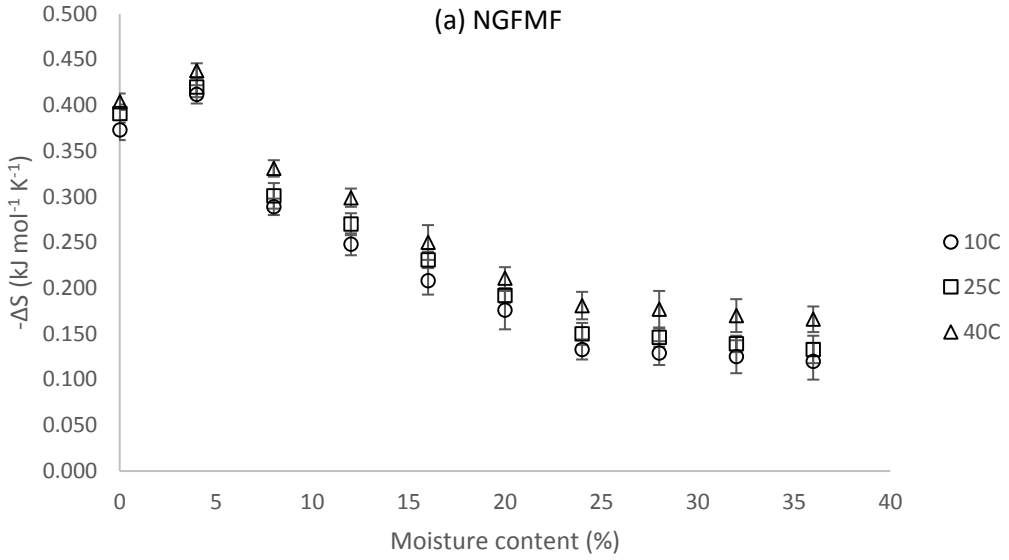

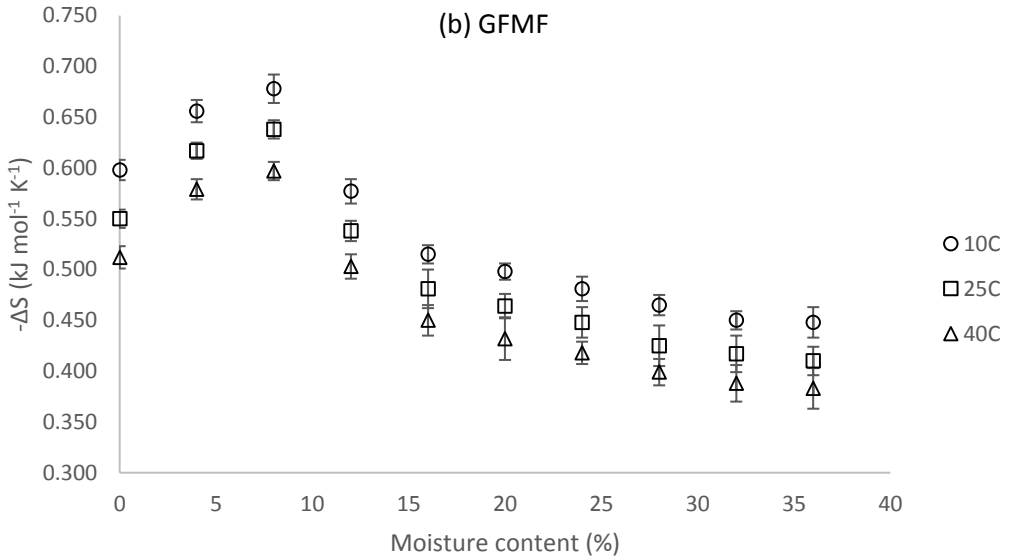

Fig. 4 Integral entropy (ΔS) as a function of moisture content of (a) NGFMF and (b) GFMF

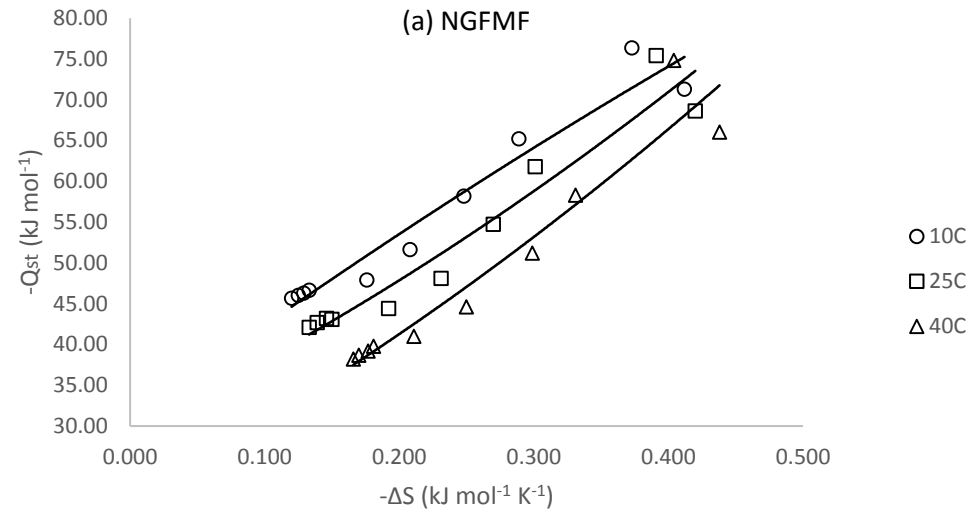

703

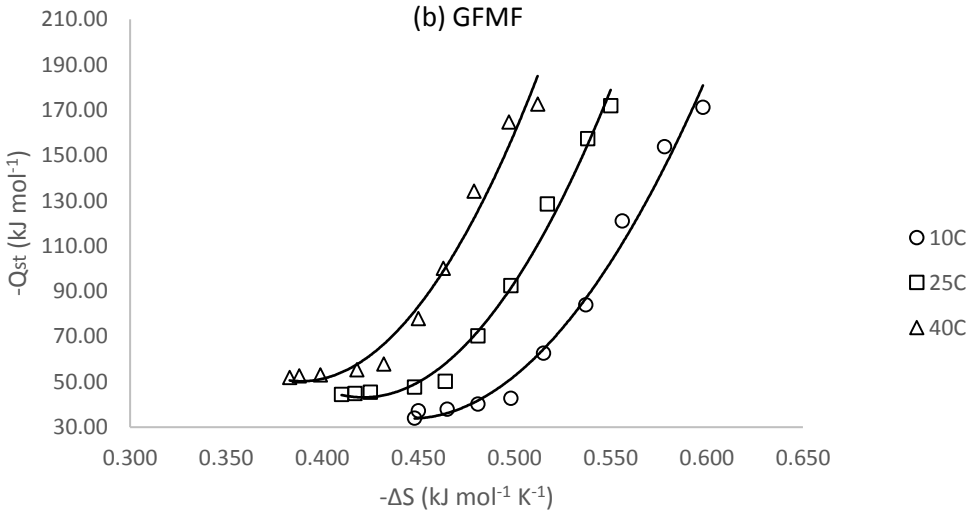

704

705 **Fig. 5** Integral enthalpy-integral entropy compensation for (a) NGFMF and (b) GFMF

706

707

708

709

710

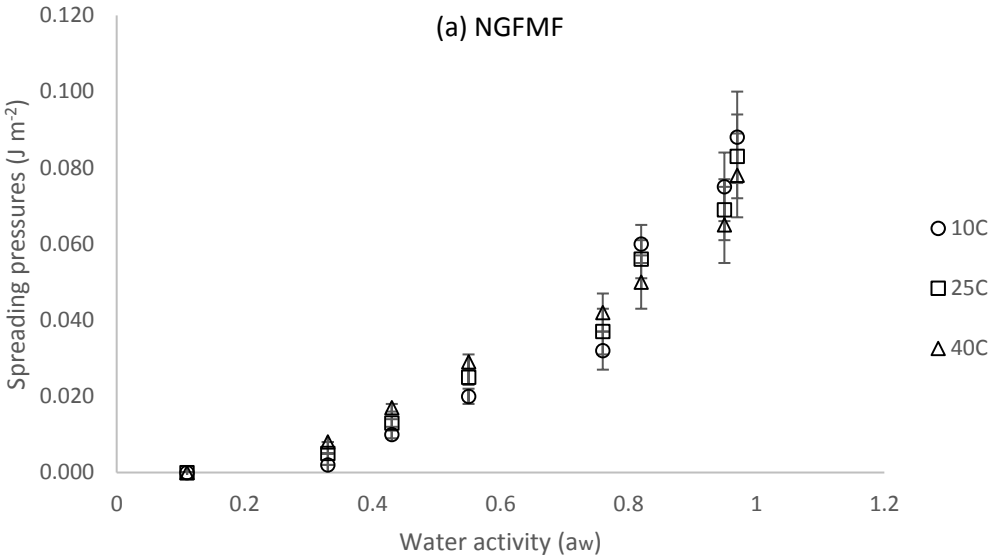

711

712

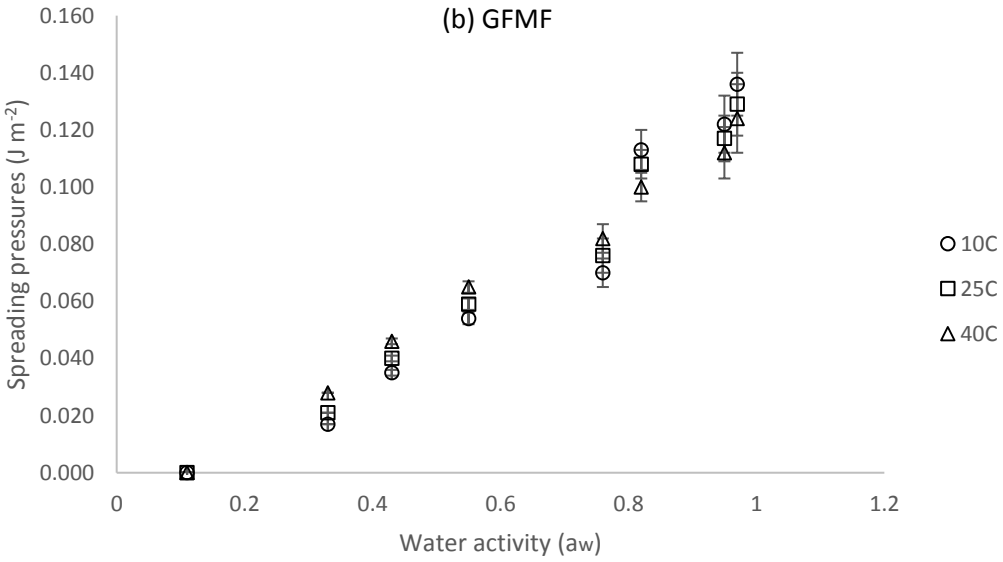

713

714 **Fig. 6** Spreading pressure isotherms as a function of water activity of (a) NGFMF and
715 (b) GFMF

716

717

718

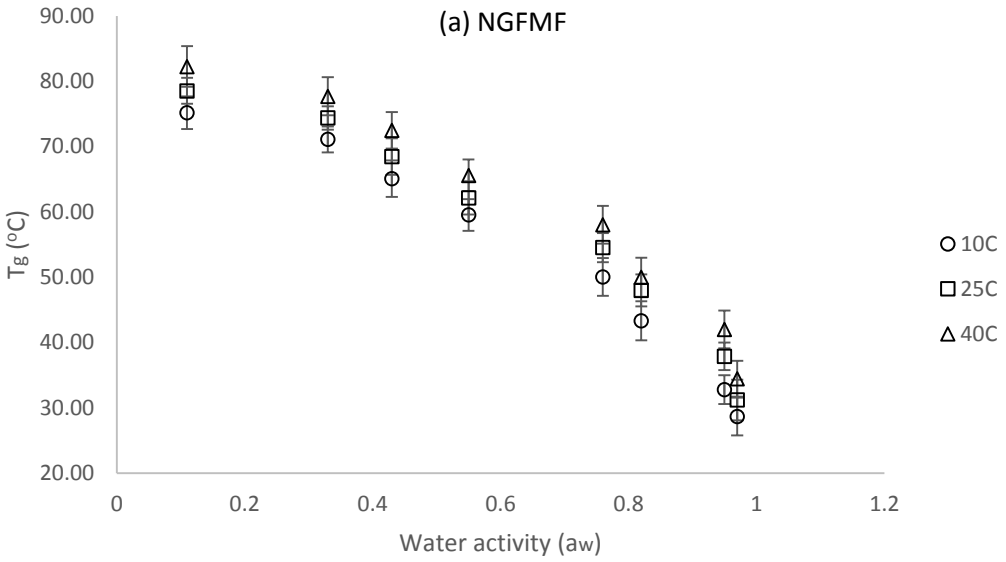

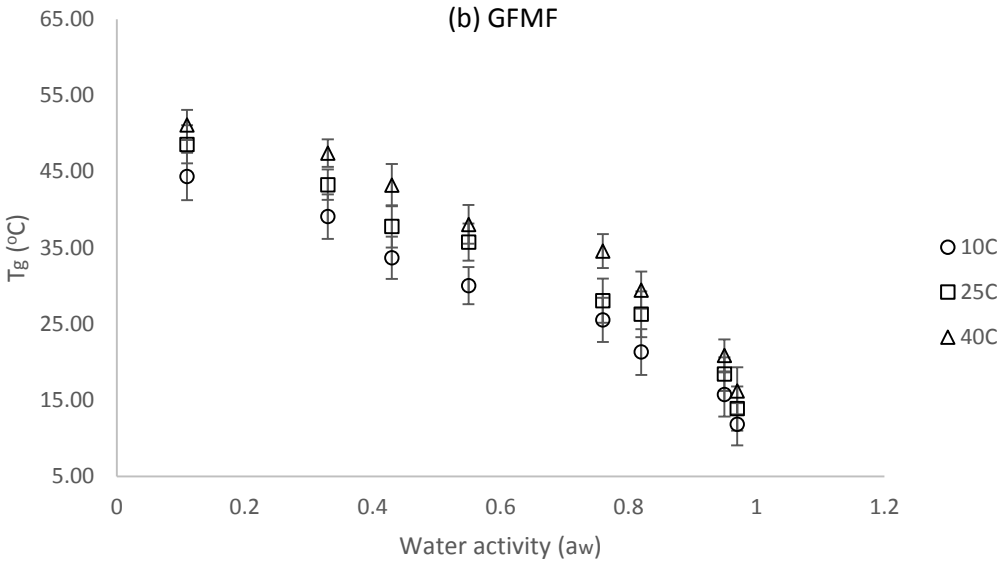

Fig. 7 Effect of water activity on glass transition temperatures of (a) NGFMF and (b) GFMF